

# **Tropical Cyclone Atmospheric Forcing for Ocean Response Models: Approaches and Issues**

**V. J. Cardone**

**and**

**A.T. Cox**

**Oceanweather, Inc.  
Cos Cob, CT, USA**

## **ABSTRACT**

The specification of tropical cyclone atmospheric forcing for ocean response models is described with emphasis on methods that are currently actively applied in basins rich in in-situ, airborne and remotely sensed meteorological data. We emphasize approaches and critical issues addressed in more detail in this workshop's special session on Tropical Meteorology. Five alternative wind fields developed for Gulf of Mexico Hurricane Katrina (2005) are applied with a third generation wave model to highlight the sensitivity of predictions of integrated properties of the wave spectrum to the wind fields, including a preliminary assessment of the sensitivity of inner core peak sea states to high frequency temporal changes in the wind forcing.

## **INTRODUCTION**

Accurate specification of wind fields for forcing ocean response models in intense extratropical storms (ETS) has been shown to be possible using a kinematic analysis approach (e.g Cardone et al., 1994; Cardone et al., 1996; Swail and Cox, 2000), whose success relies on the availability of in-situ or remotely sensed surface wind measurements. In many ocean areas, especially in the Northern Hemisphere (NH), sufficient in-situ wind data are provided for the purposes of reliable ETS reanalysis by moored buoys, offshore platforms, automatic coastal weather stations, transient ships, well exposed conventional coastal and island weather stations, active and passive microwave satellite-borne sensors and the products of the recent major

atmospheric reanalysis projects of NOAA/NCEP/NCAR and ECMWF reanalysis.

Since the launch of QuikSCAT in 1999, accurate wind field specification has become possible even over the vast reaches of the Southern Oceans (Cardone et al., 2004). The spacing and temporal resolution of in-situ observations and the footprint size (of order  $\frac{1}{4}$  degree) of the remote sensors are well suited to the temporal and spatial scale of ETS winds.

On the other hand, in a tropical cyclone (TC) conventional in-situ data sources are inadequate in spatial and temporal coverage to resolve the time evolution of the critical inner core (say the area covered by wind speeds greater than about  $\frac{1}{2}$  of the maximum wind speed) TC structure and often the available wind data themselves (especially from low mounted anemometers on small moored buoys) are not as accurate at hurricane wind speeds (say average wind speeds greater than about 30 m/s) than at lower speeds. Therefore, in most regions affected by TCs, indirect methods using a variety of models are utilized to specify the time and space evolution of the surface wind field and associated wind stress for the purposes of forcing ocean models, including wave models, hydrodynamic (HD) models used for shelf current and coastal surge prediction and 3D ocean circulation models. Only where extraordinary data types are available, such as data collected by manned or unmanned airborne probes of TCs, may specialized kinematic methods be applied.

Aircraft reconnaissance of TCs began during World War II in the Western North Pacific where it continued until 1986, and in the western

North Atlantic Ocean (NAO) and contiguous basins where it continues up to the present time. Aircraft provide invaluable additional sources of data on TC location, intensity and structure. Initially, aircraft provided basically navigational center fixes, eye characteristics from airborne radar presentation and vertically extrapolated estimates of minimum eye pressure. By the 1950s, the data included eye sounding and surface minimum pressure from eye dropsonde, flight level winds, temperature and D-value and radar images. Currently, aircraft probing of NAO cyclones provides, in addition, vertical wind profiles in the inner core from GPS dropwindsondes, remotely sensed surface wind speeds along all flight lines from the stepped frequency microwave radiometer (SFMR), Doppler radar images converted to relative wind velocity cross sections and more. These data have enabled the development and application of an additional arsenal of TC surface wind analysis approaches including kinematic analysis methods. What is notably lacking, however, is a database of accurate, over ocean in-situ measurements of the surface wind speed and direction on the most useful averaging interval (i.e. about 10 minutes). The lack of these data places a limit to the development and validation of both model-based and kinematic-based methods of surface wind analysis and, therefore, surface wind fields analyzed for even well documented storms have some uncertainty, which leads naturally to errors in modeled ocean response.

In this paper, we describe the attributes and critical deficiencies of the most widely applied methods for surface wind analysis of NAO basin TCs and explore in a preliminary way the sensitivity of wave hindcasts forced by alternative wind fields for extreme Gulf of Mexico (GOM) Hurricane Katrina (2005). The wave calculations are made with the OWI3G wave model as adapted to the GOM over the grid domain shown in Figure 1. A similar analysis that explored the sensitivity of these same wind field variants on coastal storm surge predictions was reported by Cardone and Cox (2007).

## **TROPICAL CYCLONE ATMOSPHERIC FORCING**

The hurricane marine boundary layer wind field and the hurricane inner-core sea level pressure and its gradient constitute the hurricane atmospheric forcing and the source of kinetic energy of storm-driven coastal currents, waves, storm surge and sediment transport associated with a land falling storm. The dominant forcing is the surface boundary layer wind field, which for the purposes of ocean model forcing is represented by the 10-meter elevation marine exposure wind speed and direction that represents a turbulence-filtered averaging interval (typically 30 minutes). For other purposes, estimates of gust scale “peak sustained 1-minute wind speed” and “peak 3-second gust speed” may be derived from the turbulence filtered average wind speeds through statistical gust distribution models (e.g Vickery and Skerlj, 2005). The time step at which the wind fields are prescribed should be typically 30-minutes or less and the grid spacing, at least in the inner core, should be no greater than 2 km.

### **Table 1. TC96 PBL Model Parameters**

#### **Model Physics Coefficients**

**Kh** – horizontal eddy diffusivity

**Kv**- vertical eddy diffusivity

**Zo** – aerodynamic roughness parameter

**Am, Bm, Cm** – Arya/Deardoff mean layered PBL parameterization

**fH/U\*** Ekman scale height parameterization (f is Coriolis parameter, U\* is friction velocity)

#### **Storm Specific Parameters as Function of Time**

**Eye coordinates**

**Po** central pressure

**Vg** ambient geostrophic gradient

**Rpi** scale radius

**Vf** storm motion

**Bi** peakedness parameter

**Dpi** pressure gradient parameter

**Pfar** far field pressure

**Azimuthal and temporal variability**

**H** PBL depth

**L** Obukov length

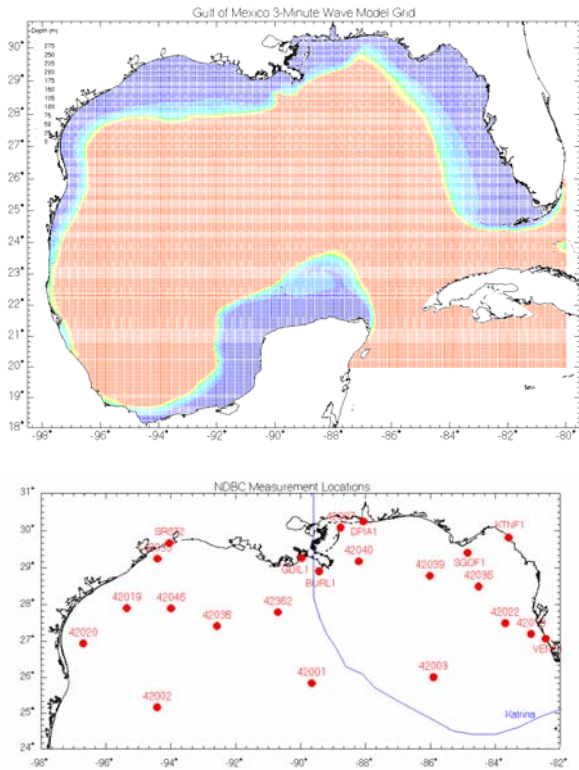


**Figure 1. Upper: OWI3G wave model grid domain showing depth contours color coded. Lower: Track of Hurricane Katrina (2005) through the Gulf of Mexico and NDBC buoys and C-MAN stations used to validate the modeled wind and wave fields.**

The main approaches to surface wind modeling in tropical cyclones may be categorized as:

- (1) Simple analytical parametric models, such as Holland (1980), Cooper (1988), Toro et al. (2004).
- (2) Steady-state dynamical such as the so-called PBL model of Chow (1970) as later developed by Cardone et al. (1976), Shapiro (1983), Thompson and Cardone (1996) and Vickery et al. (2000)
- (3) Non-Steady dynamical such as MM5 (Chen et al. 2007), GFDL (Kurihara et al., 1998) and WRF (Corbosiero et al., 2007)
- (4) Kinematical methods, most notably the NOAA National Hurricane Research Division

(NHRD) HWnd (Powell et al., 1996) and Oceanweather's (OWI) IOKA (Cox, et al., 1995).

(6) Blending method. This method involves the combination of two or more of the methods described above. For example, in a U.S. National Ocean Partnership Program (NOPP), whose objective is to provide improved real time coastal wind, waves and surge forecasts for North Atlantic Basin hurricane affecting the US East and Gulf coasts, real time PBL and HWnd solutions are blended (Graber et al., 2006). A blend approach has also been applied to hindcast Hurricane Lili (2002, Cardone et al., 2004), and Ivan (2004, Cox et al., 2005) using the solutions of reanalyzed PBL solutions and operational HWnd snapshots.

In this study, we apply representative dynamical, kinematical and blend wind fields for Hurricane Katrina (2005) in the GOM as generated both in a real time context and in a careful reanalysis mode. A PBL solution driven by simple inputs such as available in real time may also be taken as a surrogate for the parametric approach because of the simple wind field shapes produced by this method. 3-D models are not considered because they have to date been applied mainly to real time forecasting to forecast storm track or to simulations of long-term climatologies of TCs (e.g. Emanuel et al., 2006, Knutson et al., 2007) rather than to hindcasting the best possible wind field of a given historical storm.

## Steady PBL Model Wind Field

### Basic Method

The variant taken to typify the steady dynamic model approach is the widely applied PBL model usually referred to as TC96 (after Thompson and Cardone, 1996). A similar PBL model formulation was developed by Shapiro (1983) except in a cylindrical coordinate system. TC96 is an application of a theoretical model of the horizontal airflow in the boundary layer of a moving vortex (Chow, 1970). That model solves, by numerical integration, the vertically averaged equations of motion that govern a boundary layer subject to horizontal and vertical shear stresses. The equations are resolved in a

Cartesian coordinate system whose origin translates at constant velocity,  $V_t$ , with the storm center of the pressure field associated with the cyclone. Variations in storm intensity and motion are represented by a series of quasi-steady state solutions. The parameterization of the vertical shear stress for a slab PBL of arbitrary depth and thermal stratification follows the formulation of Arya (1977). The surface roughness is prescribed by a Charnock law with Charnock constant of .035 and Karman constant of 0.35. TC96 has been widely applied and validated mainly in terms of its success in forcing ocean response models. Many such studies have been reported (see e.g., Forristall et al., 1978; Cardone and Resio, 1998; Jensen et al., 2006).

### Principal Issues

**Physics.** The basic constraints of steady state physics, neglect of vertical structure and sea surface coupling can only be overcome with full 3D models such as MM5, GFDL and WRF. Apart from these simplifications of TC96 there are remaining physics uncertainties as shown in Table 1, mainly associated with the vertical shear stress parameterization. Given that the TC PBL is usually in the relatively simple state of “forced convection” in which mechanical production of turbulence dominates convective production, the Arya/Deardorff parameterization is quite robust. In light of recent tank (Donelan et al. 2004) and field evidence (Powell et al., 2003; Jarosz et al, 2007) that support the idea of a limiting value of roughness at hurricane wind speeds, the main systematic effect in TC96’s specification of peak winds in the inner core may arise from the simplified drag law adopted. Preliminary numerical experiments suggest that higher wind speeds result in the inner core with a saturation roughness law if no other parts of the PBL parameterization are modified.

**Storm Specific Parameters.** In the application of TC96 to a given TC we typically start from raw data whenever possible and carry out an intensive reanalysis of traditional cyclone parameters such as track and intensity (in terms of pressure) and then develop new estimates of the more difficult storm parameters, such as the shape of the radial pressure profile and the

ambient pressure field within which the cyclone is embedded. The time histories of all of these parameters are specified within the entire period to be hindcast. Storm track and storm parameters are then used to drive TC96 to generate a complete picture of the time-varying wind field associated with the cyclone circulation itself.

The principal challenge in the model initialization is to describe the PBL pressure gradients from a prescribed azimuthally dependent radial pressure profile, most recently expressed as a double exponential form:

$$P(r) = P_o + \sum_{i=2}^n dp_i e^{-\left(\frac{R_{pi}}{r}\right)^{B_i}}$$

where  $P_o$  is central pressure, and in its unimodal form  $dp$  is the pressure differential between the eye pressure and the storm environment,  $R_p$  is a scaling radius related to (but not in general equal to) the radius of maximum wind and  $B$  is the profile peakedness parameter, usually called Holland’s  $B$  after Holland (1980). Other assignable parameters of the planetary boundary layer (PBL) formulation include the planetary boundary layer depth,  $H$ , and stability parameter,  $L$ , and the sea surface roughness formulation. Field data studies and analyses of aircraft dropwindsonde wind profile data in the inner core of hurricanes have provided new insights and models for these characteristics.

For application to storms into which there is no aircraft reconnaissance (i.e. the vast majority of cyclones on a global basis), the input parameters are derived rather indirectly. Central pressure is usually related to Dvorak (1984) intensity estimates made by skilled interpreters of satellite imagery. The scale radius is estimated from satellite image depictions of the eye diameter and occasionally the eye wall itself. Near land, the pressure profile may be fitted directly but only for its unimodal mode and with an assumed value of  $B$ . For storms viewed by QuikSCAT, Cox and Cardone (2000) describe an inverse model approach that utilizes data outside the inner core, and which also may be applied to

estimates of the radius of 35 knot and 50 knot wind speeds as often issued by warning centers.

Where aircraft reconnaissance data are available, the central pressure is reliably known from dropsonde and the pressure profile may be fitted directly to flight level D-value legs that typically radiate out from the center along several azimuths. Thompson and Cardone (1996) described a simple software-assisted method applicable to fitting the double exponential pressure profile parameters. A more sophisticated method based on the profile form and cost function approach of Willoughby et al. (2006) is utilized in the updated tropical analysts workstation described at this workshop by Cox and Cardone (2007). However, since aircraft typically penetrate the inner core of TC at flight level of 700 mb, there is the possibility that the peakedness parameter and partitioning of the pressure differential and scale radius fitting parameters are not quite representative of the surface pressure field. At the very least there is typically a small but systematic tilt inward of the radius of maximum wind between the mid-troposphere and the surface layer. However, there does not exist yet a robust parameterization of this tilt.

In a typical application, a trial PBL model solution obtained from starting input data is compared to time histories of measured surface winds outside the inner core from buoys, and to aircraft wind speeds reduced from flight level to 10-meters using empirical ratios. Model input parameters are varied and the model solution iterated until good agreement is obtained between the modeled wind field and the better-quality wind observations available. Note, however, that buoy measurements in the inner core are extremely rare and the measurements must be viewed as suspect in storms of severe intensity (say average wind speeds above about 30 m/s). Typically, modeled cyclone tropical wind field are blended into a basin-wide field which incorporates both atmospheric modeled winds, in-situ measurements from buoys, CMAN stations, ship reports as well as satellite estimates of wind from altimeter and scatterometer instruments using a kinematical method such as IOKA. (Cox et al., 1998). Such

a wind field description can also serve as the reference for modifications of wind speed and direction in coastal waters (bays, inland lakes etc.) and over freshly inundated areas to reflect different (i.e. from nominal deep water) in-situ and upstream surface roughness (Atkinson and Wamsley, 2007).

## **HWnd.**

### **Basic Method.**

Since about 1998 a new kinematic analysis system for tropical cyclone surface wind fields known as HWnd (Powell et al., 1998) has been applied in real time to most TCs in the NAO basin by the NOAA NHRD. HWnd wind field “snapshots” are in general generated at 6-hourly intervals once regular aircraft reconnaissance missions into a given system have commenced. The analysis employs a scale controlled wind speed objective analysis system to synthesize into a continuous field, observations of winds from aircraft, SFMR, QuikSCAT, buoys, C-MAN stations, GPS dropwindsonde, offshore platforms and towers, coastal towers and the like.

### **Principal Issues.**

**Data Transformation.** The main challenge of HWnd is to first transform each observation from its intrinsic time averaging interval, and for remote sensors from their intrinsic spatial average, to the HWnd standard representation of the so-called peak “sustained” wind speed, which is defined as the peak 1-minute gust (see Powell et al., 1998). As such, HWnd wind fields should not be used for ocean forcing unless the “sustained” wind speeds are transformed to an averaging interval that has effectively filtered turbulence scale fluctuations (normally an averaging interval of at least 30 minutes satisfies this objective) and used to force an ocean model at a spatial resolution and time interval appropriate for intense hurricanes (normally the grid spacing required is 2 km or so and the time step is no greater than 30 minutes).

**Analysis Homogenization.** The considerable archive of HWnd analyses generated in real time over the past decade do not constitute a

homogeneous historical data set because the elevation and averaging interval transformations applied to the most ubiquitous data sets, namely flight level winds and SFMR, have undergone several revisions over time. The introduction of GPS winds especially has provided a basis to revise and improve the flight-level to surface wind speed ratios (Franklin et al. 2003) and the geophysical model function (GMF) used to relate SFMR emissivity to surface wind speed (Uhlhorn and Black, 2003, Uhlhorn et al., 2006). However, questions remain as to the effective averaging interval of wind speeds derived from GPS profiles or SFMR. These issues are discussed at this workshop by Powell (2007).

**Calibration.** The lack of a truly representative and accurate in-situ data base of measured winds in the inner core of a number of storms has prevented an absolute calibration and validation of the data transformations, the flight level reduction ratios and the SFMR GMF.

### **Blend**

In recent applications, HWnd snapshots have been utilized in several ways to enhance model generated wind field solution.. For example, the HWnd snapshots may be used in an “inverse-modeling” sense (see. e.g. Cox and Cardone, 2002) to find those PBL model inputs that provide a solution consistent with the HWnd patterns. In this way, quite complex and anomalous size and shape storm properties (such as, for example, the double wind maximum associated with the eye wall replacement cycle or the shelf-like radial wind profiles found in some storms) may be modeled through the double exponential representation of the PBL pressure field used in TC96. HWnd winds may also be used as a source of data that may be assimilated into a pre-existing model solution within a direct kinematic analysis using a system such as IOKA. The advantage of this approach is that it operates as an expert system and the analyst is, therefore, able to utilize off-hour and time history information, to bring in qualitative information from satellite such as TRMM. A new system of processing Doppler radar

imagery from multiple coastal sites called VORTRAC (Lee and Bell, 2007) promises to be able to monitor structural and intensity changes in the coastal zone on a time scale of minutes. This system may be especially useful for countries with extensive radar networks but no program of aircraft reconnaissance.

### **HURRICANE KATRINA WIND FIELDS**

As Katrina moved northwestward in the GOM in late August, 2005 (see track in Figure 1) it exhibited two separate bursts of intensification, the first late on August 26 which took Katrina to Category 3 intensity and the second late on the 27<sup>th</sup> and early the 28<sup>th</sup> which took Katrina to Category 5 intensity. These changes were accompanied by fairly typical structural changes in the size and degree of organization of the storm, particularly in the well monitored evolution of two distinct eye-wall replacement cycles, each of which was characterized by the formation of an outer eye wall near a radius of about 40 nm from the center and its contraction to between 15 nm and 20 nm from the center. The minimum central pressure attained by Katrina was 902 mb at about 1800 UTC August 28 with peak winds of 150 knots (this is the official NOAA Tropical Prediction Center (TPC) intensity expressed in terms of the maximum 1-minute average wind speed expected in one hour, or the so called “sustained wind”), when the center was located about 170 n mi southeast of the mouth of the Mississippi River. At maximum intensity, the radius of maximum wind was about 15 nm which is fairly large for a Category 5 hurricane. Rapid weakening of Katrina ensued over the subsequent 18 hours and Katrina, now moving almost due north, made its first Gulf landfall as a Category 3 hurricane at 1100 UTC August 29 on the northwestern coast of the Mississippi Delta. The pre-landfall weakening was accompanied by a radical change in wind structure as the inner eye-wall seen at maximum intensity collapsed as a new outer wind maximum formed, which instead of contracting maintained itself and thereby imparted a shelf-like structure to the radial distribution of wind speed, especially on the right side of the wind circulation. This

transformation is revealed vividly in comparative aircraft tail Doppler radar wind speed cross section images contained in the TPC report (2006).

Experiments were conducted with the following five wind fields in order of increasing levels of analysis:

**1. PBL Real Time (Base Case).** This case is comprised of a series of TC96 PBL solutions produced at OWI in real time to represent the analysis at 6-hourly intervals, from the estimates of eye coordinates, intensity (maximum sustained wind speed) and radii of 35 knot and 50 knot winds contained within the official advisories issued by the TPC. This wind field will likely be more accurate than a comparable wind field produced in other basins by this method because the TPC forecasters have access to reconnaissance data not available in other basins, but it nevertheless should be expected to provide a wind field of lower accuracy than a hindcast.

**2. PBL Near Real Time.** This case also represents mainly a PBL solution but with the storm track and input variables derived within a month or so after real time for the purposes of preliminary assessment of storm impact offshore on infrastructure. For the analysis of the model input parameters, a sufficient period of time has elapsed after real time to allow use of a preliminary “best track” reported by TPC in its storm report on Katrina and to fit the parameters of the exponential profile at a given analysis time by compositing all aircraft and surface measurement of surface pressure within a window of say +/-3-hours centered on the analysis time (this is not possible in real time) and imposing continuity in the PBL snapshots by being able to refer to the entire time history of the storm. A hindcast also allows some iteration of the PBL parameters after the wind field solution is compared to reliable wind data such as synoptic real time HWnd snapshots, reduced aircraft flight level winds, winds measured at buoys (within their range of reliability), from offshore platforms, and outside the inner core by QuikSCAT.

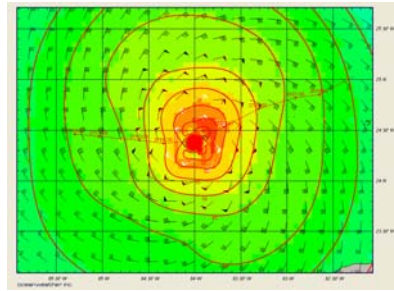
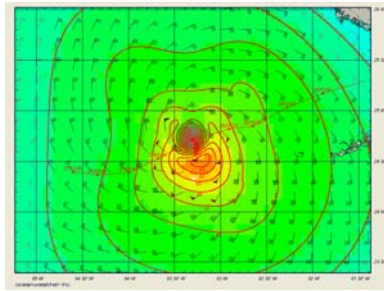
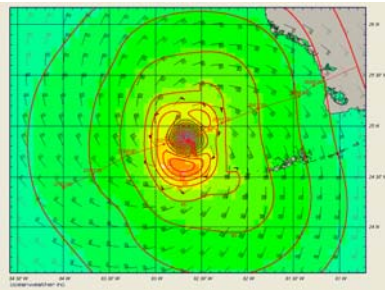
### **3. HWnd Real Time Snapshots-IPET95.**

During Katrina’s movement through the Gulf of Mexico, HWnd snapshots were produced at NHRD at 3 or 6-hourly intervals, in general. This series of analyses were turned into a continuous field, known as the IPET95 wind field because it was used in support of the US IPET study (IPET, 2007), through the application of IOKA. The HWnd analyses typically extend outward only to about 450 km from the center. The wind field outside the HWnd domain and in the periphery of the storm is specified from the 10-meter wind field analysis produced from an IOKA blend of NCEP/NCAR Reanalysis winds and available insitu/satellite wind data available in the basin. The wind field is interpolated in time to 30-minutes using a Lagrangian interpolation algorithm that conserves the azimuth and range of each grid point with respect to the translating storm center.

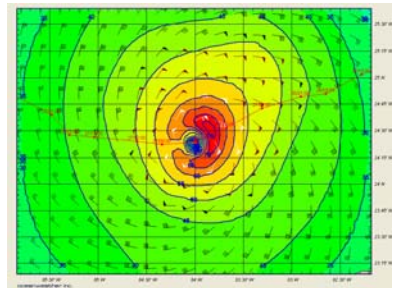
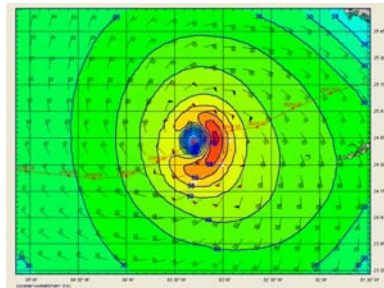
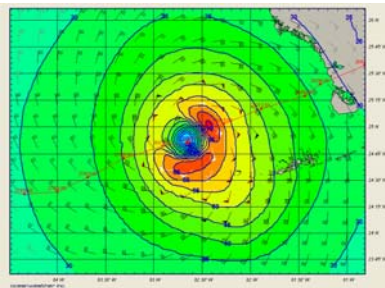
**4. HWnd Reanalyses - IPET99.** As a part of the IPET project, NHRD was commissioned to produce a set of reanalyses of Katrina during its lifecycle within the Gulf of Mexico. These analyses provide an alternative picture of the inner core of Katrina in the pre-landfall period. These HWnd analyses took advantage of a recalibration of the SFMR wind dataset and aircraft reduction methodology used to run the HWnd system (Powell, personal communication)

**5. MMS Blend.** This wind field is a blend of HWnd reanalyzed snapshots and a final set of PBL solutions generated long after real time. The final blending involves kinematic analysis techniques that are by no means restricted to the outer core. In the kinematic approach both HWnd and PBL solutions may be overridden if supported by credible wind data and to impose time continuity in the evolution of major wind field features such as the radius and quadrant of the maximum wind, such as shown for example in Figure 2. This blend solution is the only wind field of those referenced here that appears to fully capture the rapid decay and expansion of

HRD IPET 99%



OWI IOKA Solution

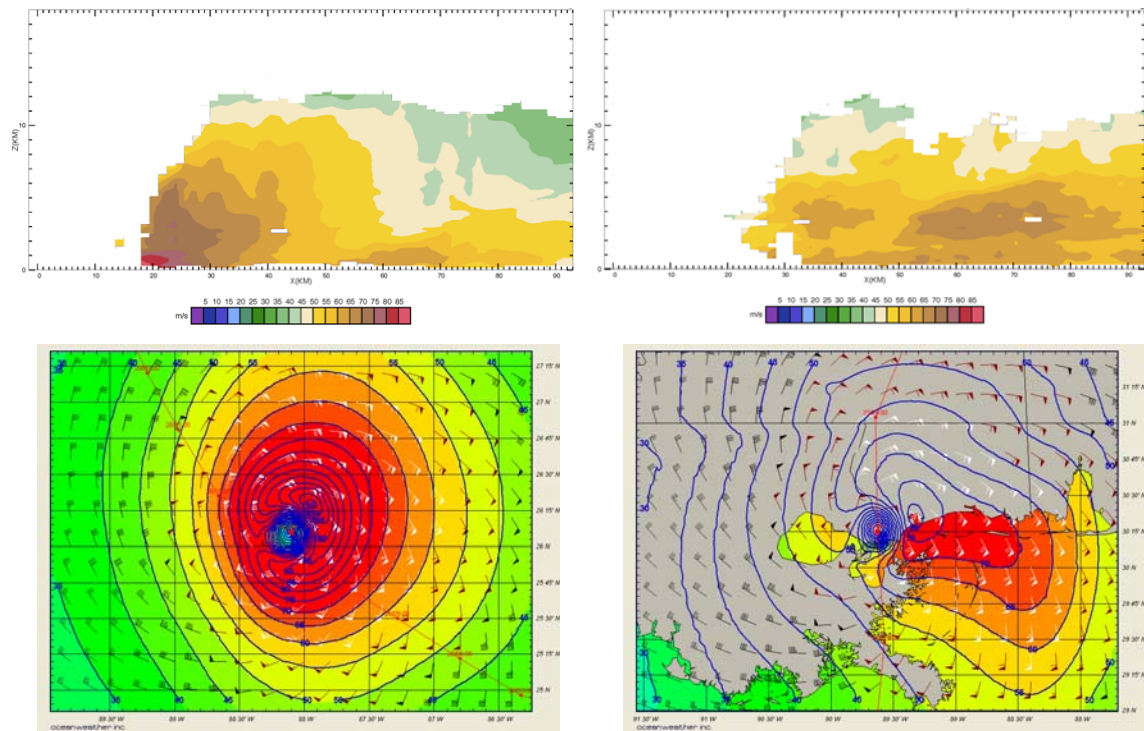


26/18 GMT

27/00 GMT

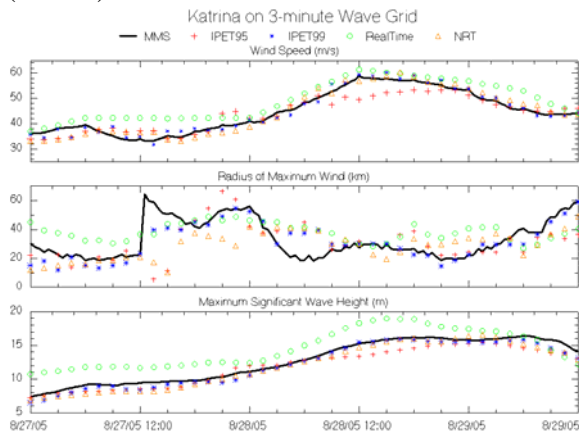
27/06 GMT

**Figure 2. Comparison of HWnd (top) and IOKA (bottom; from "MMS blend" wind field) generated wind isotachs (knots, 30-min, 10m) for indicated part of history of Katrina 2005.**



**Figure 3. Upper panels show vertical cross section of the wind field of Hurricane Katrina derived from airborne tail Doppler radar images at 1800 UTC August 25, 2005 (left) when the storm was at Category 5 intensity and at 1200 UTC August 26, 2005 (right) shortly after Katrina’s second landfall (from TPC, 2006). Lower panels: show “MMS blend” wind field snapshots corresponding to the times of the upper panels.**

the surface wind field in the 18-hour period before landfall as shown in Figure 3.. This wind field is further documented and validated by Cardone et al. (2007), who describe a definitive ocean response hindcast study of Katrina in the GOM supported by the US Minerals Management Service (MMS). That study was carried out to support engineering studies of damage and loss of offshore infrastructure. This “MMS” wind field has also been used to drive a very high resolution adaptation of ADCIRC for validation of coastal surge modeling and subsequent coastal flood risk reassessment along the GOM coast in studies supported by the US Federal Emergency Management Administration (FEMA).



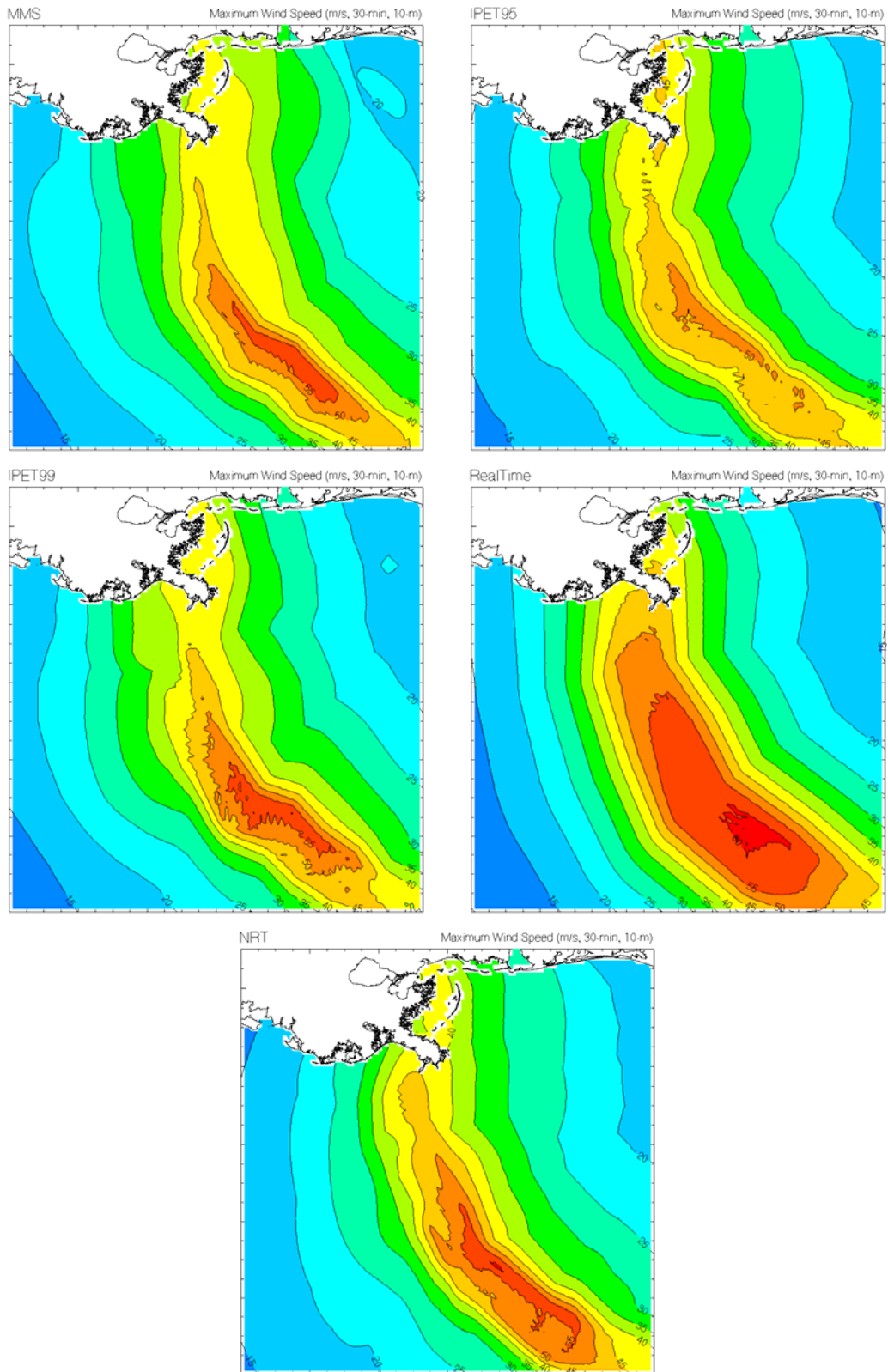
**Figure 4 Timeseries comparison of wind speed (top, m/s, 30-min, 10m), radius of maximum wind (km, middle) and maximum significant wave height (m) on common wave grid for 5 alternative wind fields.**

Figure 4 shows, for all wind fields, the time history of the modeled radius of maximum wind,  $R_{max}$ , and maximum wind speed (30-minute average at 10-meter elevation over water) during the period that the storm was in the GOM. The bold line represents the MMS Blend solution which is the wind field that most faithfully tracks all available estimates of  $R_{max}$  and  $V_{max}$  from flight level data. The flight level  $R_{max}$  was not modified though it should be expected that due to eye-wall tilt the surface  $R_{max}$  may be smaller than the flight level  $R_{max}$ .

There is a remarkable degree of variability in the solutions of these important properties of the inner core of Katrina. The real time solution is the most energetic, probably because the Kraft transformation provided an eye-pressure estimate from the TPC “best track” peak wind that was lower than the true central pressure. The IPET99 and MMS Blend solutions best represent the rapid expansion of  $R_{max}$  before landfall.

There is a large difference in peak wind speed between the real time and reanalyzed HWnd snapshots over about an 18-hour period straddling the time of peak storm intensity. The later IPET99 peak winds are nearly 10 m/s higher than in IPET95. This change probably reflects a change in the flight level-surface wind speed reduction factor between the two analyses (this ratio is a user selectable feature of the HWnd user interface). The MMS wind field tracks the IPET99 winds closely except immediately before landfall because the blending process highly weights the HWnd in the inner core. Before landfall the MMS wind field was strongly influenced by rapid change in the airborne tail Doppler radar cross section representation of the wind field before landfall (see Figure 3) as noted above (see also Cardone et al. 2006 and TPC, 2005). Finally, we note that the fast-response near real time PBL solutions comes remarkably close to the final MMS wind field in terms of  $V_{max}$  and associated  $R_{max}$ .

Figure 5 compares the alternative wind fields as color contours of the envelope of maximum wind speed fields. The real time wind field appears to be too energetic and too broad in the inner core relative to the MMS and both IPET solutions. The near real time PBL winds are close to the IPET solutions. The MMS blend solution shows more broadening of the wind field to the right of the center before landfall as suggested by the airborne Doppler radar wind cross section.



**Figure 5 Maximum wind speed (m/s, 30-min, 10m) from five alternative wind fields**

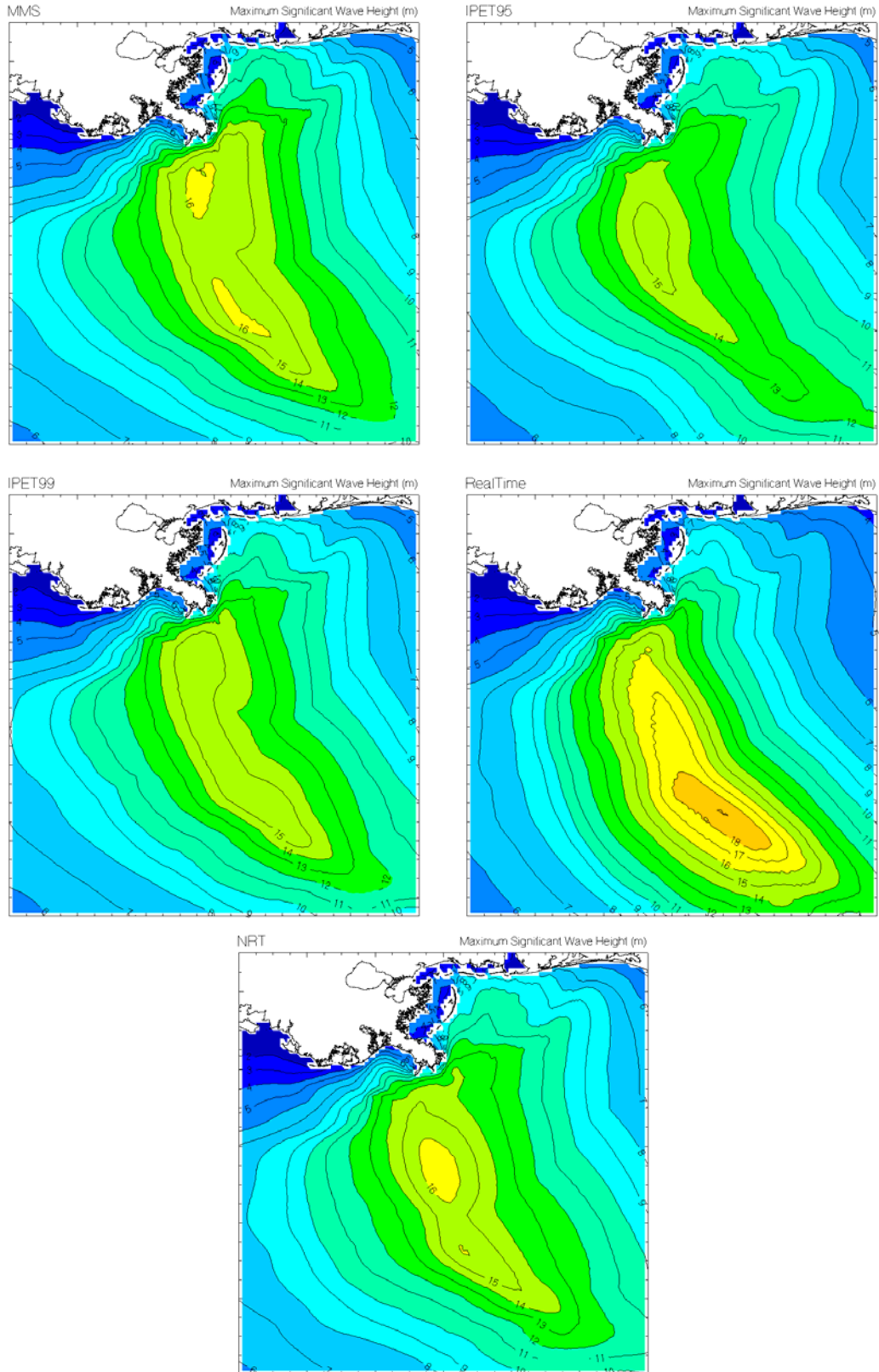


**Figure 7 Maximum hindcast significant wave height (m) from five alternative wind fields**

## WAVE RESPONSE TO ALTERNATIVE WIND FIELDS

### Wave Model

The alternative wind fields are each used to simulate the evolution of the sea state in Hurricane Katrina in the GOM using a third-generation wave model developed at OWI (OWI3G). The model grid is shown in Figure 1. The source term balance of OWI3G follows the formulation of WAMD1 (1988) with the important exceptions that OWI3G includes a linear excitation term (A term) in its atmospheric input and accounts for a second mode of interaction in the discrete interaction approximation (DIA) to the non-linear source term. Rather than adopt the standard WAM linear drag law to convert wind speed at 10 meters to friction velocity for the wave model atmospheric input source term, OWI3G adopted a form that approaches a limiting value of about  $2.2 \times 10^{-3}$  at a wind speed of about 30 m/s. Documentation of the source terms and drag law of OWI3G is given in Khandekar et al.(1994), Forristall and Greenwood (2000). The propagation scheme is described by Greenwood Cardone and Lawson (1985).

### Results

Figure 3 shows the time evolution of the maximum significant wave height for each wind field. The real time solution is most energetic because of the bias in the peak wind speed noted above. The other solutions are quite similar. The trend in the peak HS tracks the trend in the wind speed more closely than it does the trends in Rmax. HS changes tend to lag the peak wind speed when the storm is intensifying whereas when the storm is weakening the growth of HS is interrupted but not reversed, as shown also in Figure 6 which compares, for the MMS blend hindcast only, hourly (also smoothed to 3- and 6-hourly) changes in peak wind speed, associated Rmax and peak HS.

Figure 7 compares the alternative OWI3G solutions in terms of color contours of the

envelope of the peak modeled HS. The real time run yields the highest peak HS of about 19 m when the storm attained Category 5 intensity but the radial extent of high seas was more limited than all of the non-real runs. Both IPET runs yield the lowest peak HS, just short of 16 m while the MMS wind field gives a peak HS of nearly 17 m not only at peak intensity but also as the center of Katrina approached the MS delta at which point shallow water effects began to affect the solution. To the left of the track the IPET99 and MMS solutions are essentially identical while to the right of the track the MMS wind field allows an increase of about 1 m in peak HS to the right of the delta.

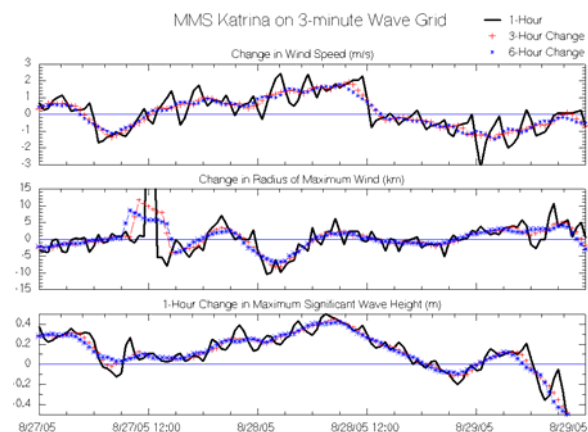


**Figure 6. 1, 3 and 6 hourly changes in wind speed (top, m/s), radius of maximum winds (middle, km) and maximum significant wave height (bottom, m).**

Figure 7 shows comparisons of time histories of the measured and modeled HS and TP at NOAA buoy 42040, which is the buoy that experienced the highest wind speed and sea state measured in Katrina. All wind fields except MMS Blend track the buoy measured wind speed (adjusted to 10 –meters) quite well within 24-hours of the peak, except for the NRT wind field, which tracks lower than the buoy on the approach to and decay from the inner core representation of the wind fields and the MMS Blend wind field, which tracks significantly above the buoy wind speed from about 15-hours before the peak to about 6 hours after the peak. It is interesting that during this time, this small discus buoy is measuring HS in excess of about

8 m. It is to be expected that the IPET95 wind fields, which also influenced the NRT TC96 wind field, and the IPET99 wind field, agree with the buoy history because the buoy winds are naturally assimilated into the wind field analysis process. The MMS Blend analysis is not constrained by the buoy winds because we believe (and have as yet unpublished evidence) that wind speeds from small discus become increasingly biased low in sea states above 8 m and/or ambient wind speeds of greater than about 30 m/s. The HS time history indicated that all of the wind fields that faithfully track the reported wind speed at the buoy underestimate the wave height from about 12-hours before the peak to about 6 hours after the peak. The MMS Blend hindcast agrees best with the buoy time history except for the 6-hour period straddling the peak.

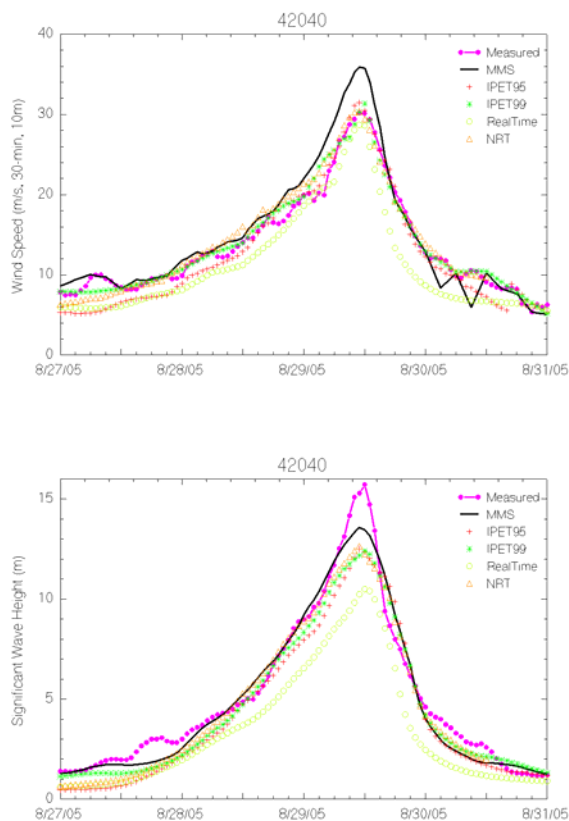


**Figure 8 Comparison of measured winds (top) and waves (bottom) from NOAA buoy 42040 vs. 5 alternative wind/wave fields during Katrina 2007**

It is not yet clear why OWI3G driven by MMS Blend underestimated the peak HS at 42040, but it may be indicative of a bias arising in the wave model source term balance tuning rather than a wind field effect. Obviously, more research is needed to isolate the source of this bias. Interestingly, a negative bias in the peak HS hindcast was also seen with this hindcast technology in Hurricane Ivan (2004) at this same buoy. This issue is also discussed by Forristall (2007) at this conference.

Table 2 gives statistical differences for each run between the model predictions and the buoy data for peaks only of wind speed and associated wind direction, and wave height and associated period and mean direction. For wind speed, the correlation coefficient (CC) is lowest (at 0.78) for NRT and best (at 0.88) for MMS Blend. For wave height, the poorest agreement (at 0.59) is seen for NRT again and the best agreement is for MMS Blend (0.88) and IPET95 (0.89). MMS Blend also exhibits the smallest bias in HS and TP. For HS, the scatter index varies from 0.34 for NRT to 0.18 for MMS Blend and IPET95.

## DISCUSSION

Given the copious in-situ, airborne and satellite monitoring of GOM TCs, carefully hindcast fields using either steady state PBL or kinematic methods can provide rather skillful hindcasts of sea state in the inner core even for a catastrophic event such as Katrina. Only the wind field produced in real time from estimates of maximum wind speed and storm size contained in warning center advisories differed significantly from the hindcasts. Skill in real time forecasts of changes in storm intensity and structure is very low so errors in real time sea states will be limited in skill until 3D models have advanced to the point where real skill in forecasting intensity and structural changes in the surface wind field is realized. However, it is hard to envision operational considerations (other than of course infrastructure designs) that would require differentiation of a peak forecast of sea state of 16 m from a forecast of 18 m.

**Table 2. Peak-to-Peak wind and wave statistics for all NDBC buoys/CMAN stations during Katrina 2005.**

	Num	Mean	Mean	Diff	RMS	Std	Scat	Corr
	Pts	Meas	Hind	(H-M)	Error	Dev	Index	Coeff
	-----	-----	-----	-----	-----	-----	-----	-----
<b>MMS</b>								
Wind Spd. (m/s)	19	23.3	24.2	0.94	4.64	4.54	0.19	0.88
Wind Dir. (deg)	19	132.5	147.7	6.01	N/A	23.21	0.06	N/A
Sig Wave Ht (m)	8	8.3	8.4	0.07	1.54	1.54	0.18	0.88
Wave Period (s)	8	8.6	8.4	-0.25	2.68	2.67	0.31	0.46
Wave Dir (deg)	6	141.1	155.4	-29.74	N/A	65.43	0.18	N/A
<b>IPET95</b>								
Wind Spd. (m/s)	19	23.3	22.7	-0.57	5.37	5.34	0.23	0.85
Wind Dir. (deg)	19	132.5	156.2	8.16	N/A	25.21	0.07	N/A
Sig Wave Ht (m)	8	8.3	7.7	-0.60	1.63	1.51	0.18	0.89
Wave Period (s)	8	8.6	8.2	-0.45	2.63	2.59	0.30	0.56
Wave Dir (deg)	6	141.1	167.0	-26.76	N/A	70.85	0.20	N/A
<b>IPET99</b>								
Wind Spd. (m/s)	19	23.3	23.2	-0.09	4.78	4.77	0.20	0.83
Wind Dir. (deg)	19	132.5	148.6	5.68	N/A	24.57	0.07	N/A
Sig Wave Ht (m)	8	8.3	8.0	-0.25	1.72	1.70	0.20	0.85
Wave Period (s)	8	8.6	8.2	-0.39	2.71	2.68	0.31	0.49
Wave Dir (deg)	6	141.1	159.8	-27.02	N/A	68.34	0.19	N/A
<b>RealTime</b>								
Wind Spd. (m/s)	19	23.3	23.3	-0.03	6.69	6.69	0.29	0.78
Wind Dir. (deg)	19	132.5	142.8	7.78	N/A	27.72	0.08	N/A
Sig Wave Ht (m)	8	8.3	7.3	-0.98	2.97	2.81	0.34	0.59
Wave Period (s)	8	8.6	7.9	-0.69	2.79	2.70	0.31	0.43
Wave Dir (deg)	6	141.1	164.8	-39.21	N/A	74.42	0.21	N/A
<b>NRT</b>								
Wind Spd. (m/s)	19	23.3	22.3	-0.96	5.32	5.24	0.22	0.83
Wind Dir. (deg)	19	132.5	153.6	9.75	N/A	23.17	0.06	N/A
Sig Wave Ht (m)	8	8.3	8.2	-0.15	1.71	1.71	0.20	0.85
Wave Period (s)	8	8.6	8.3	-0.26	2.71	2.70	0.31	0.46
Wave Dir (deg)	6	141.1	155.8	-26.42	N/A	64.83	0.18	N/A

Uncertainties in wind field hindcast by application of a steady state PBL approach arise mainly in uncertainty in specification of the input parameters. Storms with the same Saffir-Simpson Scale Number, same central pressure, and roughly comparable sizes and forward velocity in the same geographic area can have significantly different maximum winds and consequent ocean response. Within the context of steady state PBL models, uncertainty in modeling this variability stems mainly from natural variability in the shape of the radial pressure profile, some effects of which may be approximated by the peakedness parameter, B,

of the exponential pressure profile. In general, however, storms may exhibit even more complex radial pressure and wind distributions, and may require double exponential representation of the radial pressure profile, as introduced in TC96. The new sectionally continuous parametric representation of radial wind distributions of Willoughby and Rahn (2006) is an important advance in this regard.

Apart from failure to model non-steadiness and the inability to model transient convectively induced changes in the inner core wind field (e.g. diurnally varying convective bursts) the scaling of peak surface winds in a steady PBL model in terms of the pressure field is most sensitive to the specification of surface friction though the drag or surface roughness parameterization. Recent studies make a compelling case for saturation of the drag coefficient to values of the order of  $2.0 \times 10^{-3}$  at wind speeds of about 30 m/s and a possible decrease thereafter at even higher wind speeds (Powell et al., 2003; 2007; Donelan et al. 2004; Chen et al., 2007; Jarosz et al., 2007). However, it remains to be demonstrated that a similar saturation effect occurs in shallow water.

Uncertainty in the kinematically based methods arise mainly in uncertainties in the process of homogenization of the various in-situ and remotely sensed data to reflect over-water surface winds at a selected averaging interval. The authors favor homogenization of the data to a wind speed averaging interval of 30-minutes, which should be the interval most suitable for forcing ocean models. The HWnd method favors homogenization of winds to a stochastic wind variable, namely the 1-minute peak sustained wind speed and associated direction. HWnd analyses, therefore, need to be transformed before they are used to drive ocean response models.

The data homogenization process is sensitive to assumptions regarding the accuracy of the vertical wind shear model used to reduce flight level winds to 10-meters, the calibration of the geophysical model function (GMF) used to convert SFMR emissivity to surface wind speed, the treatment of GPS dropwindsondes, which at

best yield a random (not peak) 1-minute average wind speed as the probe falls through the lower 150 meters of the surface boundary layer, and possible bias in in-situ sensors associated with buoy motion, and for coastal stations, less than ideal marine exposure. As noted in the introduction, these aspects of data processing and transformation have not stabilized and continue to evolve. As a result, the existing database of TC wind fields produced in real time or shortly thereafter do not necessarily provide a consistent, homogeneous archive of the wind fields of historical storms.

What are sorely needed are absolutely reliable and unbiased measurements of the surface wind speed and direction in the inner core of intense TCs by high quality well exposed anemometers whose output is recorded at high frequency. Winds measured by the larger moored buoys, such as the NOAA NDBC 10-meter and 12-meter discus buoys appear to satisfy as do winds from top of derrick mounted anemometers on offshore platforms. Newer potential sources of high-quality in-situ winds include the highly instrumented meteorological towers installed on slender monopods at planned and operational offshore wind energy farm arrays, dedicated metocean towers such as the KORDI tower in the Sea of Japan hold the promise to build the in-situ database required over time. In the GOM there is a need to better instrument offshore platforms with recording anemometers placed on the top of the drilling derrick and provided with power even during times when the platform is shut-in and evacuated during cyclone threats..

There is no aircraft reconnaissance of TCs in most part of the globe, which removes output from eye radiosonde, high frequency flight level wind, D-value and temperature sampling, GPS dropwindsonde, SFMR and airborne Doppler radar from the arsenal of data available to analyze TC surface wind fields. Fortunately, research continues into the application of satellite information in increasingly sophisticated ways. Olander and Velden (2007) report on an advanced Dvorak technique that greatly reduces the subjectivity of estimating TC intensity from geostationary satellite (GEOS) imagery while maintaining the skill of the

method when applied by the most experienced practitioners of this method. Kossin et al., (2007) report an objective method that can provide reliable estimates of  $R_{max}$  from Infrared GOES imagery and even extend the method to the specification of the tangential wind profile in the inner core.

We have already noted how surface winds outside the inner core from an active microwave scatterometer, such as QuikSCAT may be used in an inverse modeling approach to estimate the parameters of the exponential profile (Cox and Cardone, 2000). Wimmers and Velden (2007) describe an advanced visualization approach that may be applied to passive microwave sensors on low earth orbit satellites to diagnose the continuous evolution of TC features such as eye wall character and diameter, secondary eye wall formation and inward migration (as part of the eye wall replacement cycle) from intermittent sampling typical of orbiting satellites.

Of course, it is to be expected that satellite data alone may not yield some of the more subtle characteristics of the inner core of TC such as the peakedness of the profile and the details of the asymmetry of the surface wind maximum. Hopefully, intensive studies of TCs in the NA basins will yield reliable synoptic-climatological models for the mean properties of these secondary features. Uncertainties in these mean properties are discussed at this workshop by Vickery (2007).

Finally, for shallow water wave prediction and coastal storm surge modeling in particular, more research needs to be carried out to understand the cause of the sharp structural and intensity changes in the wind field sometimes seen as in the 12-24 hour period just before landfall in Katrina and other storms. Models of the rate of increase of central pressure in the post-landfall period (e.g. Vickery, 2005) need to be extended to the pre-landfall period. TC characteristic pre-landfall effects will no doubt have large regional and perhaps latitudinal variations. Longer term, it is to be expected that coupled ocean-atmosphere 3D models will naturally yield understanding of these changes and lead to improved forecasts. Promising initial results of

realistic numerical simulations of actual hurricanes with 3D models are reported at this workshop by Chen (2007), Davis (2007) and Knutson (2007).

## ACKNOWLEDGEMENTS

This study is carried out under the U.S. Army Corps of Engineers MORPHOS project, supported in part at OWI through a contract with Woolpert, Inc. and the U.S. Army Engineer District (Philadelphia) Award W912BU-07-P-0232.

## REFERENCES

Arya, S. P. S, 1977: Suggested revisions to certain boundary layer parameterization schemes used in atmospheric circulation models. *Mon. Wea. Rev.*, 105, 2, 215-227..

Cardone, V. J., W. J. Pierson, and E. G. Ward. 1976: Hindcasting the directional spectrum of hurricane generated waves. *J. of Petrol. Tech.*, 28, 385-394.

Cardone, V. J., H. C. Graber, R. E. Jensen, S. Hasselmann, M. J. Caruso 1994. In search of the true surface wind field in SWADE IOP-1: Ocean wave modelling perspective. *The Global Atmosphere and Ocean System*, 3, 107-150.

Cardone, V. J., R. E. Jensen, D. T. Resio, V. R. Swail and A. T. Cox 1996. Evaluation of contemporary ocean wave models in rare extreme events: Halloween storm of October, 1991; Storm of the century of March, 1993. *J. of Atmos. and Ocean. Tech.*, 13, 198-230.

Cardone, V. J., A. T. Cox, K. A. Lisaeter and D. Szasbo, 2004: Hindcast of Winds, Waves and Currents in Northern Gulf of Mexico in Hurricane Lili (2002). Offshore Technology Conference, Houston, TX, 3-6 May, 2004. Paper OTC 16821.

Cardone, V. J and D.T. Resio. Assessment of Wave Modeling Technology. Fifth International Workshop on Wave Hindcasting and Forecasting, 26-30 January, 1998, Melbourne, FL.

Cardone, V. J. A. T. Cox and G. Z. Forristall, 2007: Hindcast of winds, waves and currents in Hurricanes Katrina (2005) and Rita (2005). Offshore Technology Conference, Houston, TX, 30-April – 3 May, 2007. Paper OTC 18652.

Cardone, V. J. and A. T. Cox, 2007: Tropical cyclone wind forcing for surge models: critical issues and sensitivities. First JCOMM International Storm Surge Symposium. Seoul, Korea. October, 2007..

Chow, S. H., 1970: A study of the wind field in the planetary boundary layer of a moving tropical cyclone. MS Thesis, School of Engineering and Science, New York University, New York, NY.

Chen, S.S., J. F. Price, W. Zhao, M. A. Donelan and E. J. Walsh, 2007: The CBLAST-Hurricane Program and the next generation fully coupled atmosphere-wave-ocean models for hurricane research and prediction. *B. Amer. Meteor. Soc.*, 88, (March), 311-317.

Chen, S., 2007: CBLAST program of coupled high resolution hurricane model. 10<sup>th</sup> International Workshop on Wave Hindcasting and Forecasting and Coastal Hazard Symposium, North Shore, Hawaii, November 11-16, 2007.

Cooper, C. K., 1988: Parametric model of hurricane generated winds, waves and currents in deep water. OTC 5738. Offshore Technology Conference, May, 1988, Houston, TX.

Cooper, C. and J. Stear, 2006: An historical perspective of hurricane intensity in the Gulf of Mexico during 2004-2005. Offshore Technology Conference, Houston, TX.

Corbosiero, K.L., W. Wng, Y. Chen, J. Dudhia and C. Davis, 2007: Advanced research WRF high frequency model simulations of the inner core structure of Hurricanes Katrina and Rita (2005). 8<sup>th</sup> WRF User's Workshop. National Center for Atmospheric Research, Boulder, CO., June 11-15, 2007.

Cox, A. T., V. J. Cardone, F. Counillon and D. Szabo, 2004: Hindcast of Winds, Waves and Currents in Northern Gulf of Mexico in Hurricane

Ivan (2004). Offshore Technology Conference, Houston, TX, 2-5 May, 2005. Paper OTC 17736.

Cox, A.T. and V.J. Cardone, 2000: Operational System for the Prediction of Tropical Cyclone Generated Winds and Waves 6<sup>th</sup> International Workshop of Wave Hindcasting and Forecasting, November 6-10, 2000, Monterey, California.

Cox, A.T., J.A. Greenwood, V.J. Cardone and V.R. Swail, 1995. An interactive objective kinematic analysis system. Proceedings 4th International Workshop on Wave Hindcasting and Forecasting, October 16-20, 1995, Banff, Alberta, p. 109-118.

Cox, A.T. and V.J. Cardone 2007. Specification of Tropical Cyclone Parameters from aircraft reconnaissance measurements. 10<sup>th</sup> International Workshop on Wave Hindcasting and Forecasting and Coastal Hazard Symposium, North Shore, Hawaii, November 11-16, 2007.

Davis, C. and G. Holland, 2007: Realistic simulations of intense hurricanes with the NCEP/NCAR WRF modeling system. 10<sup>th</sup> International Workshop on Wave Hindcasting and Forecasting and Coastal Hazard Symposium, North Shore, Hawaii, November 11-16, 2007.

Dvorak, V. F., 1984: Tropical cyclone intensity analysis using satellite data. NOAA Tech. Rep. NESDIS 11, 47pp.

Donelan, M.A., B. K. Haus, N. Reul, W. J. Plant, M. Stiassnie, H. C. Graber, O. B. Brown, E. S. Saltzman, 2004: On the limiting aerodynamic roughness of the ocean in very strong winds. *Geophys. Res. Lett.*, 31, L18306, doi:10.1029/2004GL019460.

Emanuel, K., S. Raveal, E. Vivant and C. Risi, 2006: A statistical deterministic approach to hurricane risk assessment. *BAMS*, March, 299-314

Forristall, G. Z., E. G. Ward, V. J. Cardone, and L. E. Borgman. 1978. The directional spectra and kinematics of surface waves in Tropical Storm Delia. *J. of Phys. Oceanog.*, 8, 888-909.

Forristall, G. Z. and J. A. Greenwood, 2000: Directional spreading of measured and hindcasted

wave spectra. 6<sup>th</sup> International Workshop on Wave Hindcasting and Forecasting, November 6-10, 2000, Monterey, CA. Preprints available at <http://www.waveworkshop.org>.

Forristall, G. Z., 2007: Comparing hindcasts with wave measurements during Hurricanes Lili, Ivan, Rita and Katrina. 10<sup>th</sup> International Workshop on Wave Hindcasting and Forecasting and Coastal Hazard Symposium, North Shore Oahu, Hawaii, November 11-16, 2007.

Franklin, J. L., M.L. Black and K. Valde, 2003: GPS dropwindsonde wind profiles in hurricanes and their operational considerations. *Wea. Forecasting*, 18, 32-44.

Graber, H. C., V. J. Cardone, R. E. Jensen, D. N. Slinn, S. C. Jagen, A. T. Cox, J. M. D. Powell and C. Grassl, 2006: Coastal forecasts and storm surge predictions for tropical cyclones: A timely partnership. *Oceanography*, 19, 1(March), 130-141.

Greenwood, J. A, V. J. Cardone and L. M. Lawson, 1985: Intercomparison test version of the SAIL wave model. In *Ocean Wave Modeling*, The SWAMP Group, Plenum, Cahp. 22, 221-233.

Holland, G. J., 1980: An analytic model of the wind and pressure profiles in hurricanes. *Mon. Wea. Rev.* 108,1212-1218.

IPET, 2007. Performance Evaluation of the New Orleans and Southeast Louisiana Hurricane Protection System. U.S. Corps of Engineers <http://ipet.wes.army.mil>

Jarosz, E., D. A. Mitchell, D. W. Wang and W. J. Teague, 2007: Bottom-up determination of air-sea momentum exchange under a major tropical cyclone. *Science*, 315, 1707-1709.

Jensen, R.E., V.J. Cardone and A.T. Cox, 2006: Performance of Third Generation Wave Models in Extreme Hurricanes. 9th International Wind and Wave Workshop, September 25-29, 2006, Victoria, B.C.

Khandekar, M.L., R. Lalbeharry and V.J. Cardone, 1994. *The Performance of the Canadian Spectral Ocean Wave Model (CSOWM) During the Grand*

*Banks ERS-1 SAR Wave Spectra Validation Experiment*. Atmosphere-Ocean, **32**, 1, 31-60.

Knutson, T. R., J. J. Sirutis, S. T. Garner, I. M. Held and R. E. Tuleya, 2007: Simulations of the recent multidecadal increase of Atlantic hurricane activity using an 18-km-grid regional model. *BAMS*, 88, 10 (October), 1549-1565.

Kolar, R. L., Gray, W. G., Westerink, J. J., and Luettich, R. A. Jr. (1994a). "Shallow water modeling in spherical coordinates: Equation formulation, numerical implementation, and application." *Journal of Hydraulic Research*, 32(1), 3-24

Kossin, J.P., J. Knaff, H. Berger, D. Herndon, T. Cram, C. Velden, R. Murnanne and J. Hawkins. Estimating Hurricane Wind Structure in the Absence of Aircraft Reconnaissance. *Weather and Forecasting*, Vol. 22, Issue 1, pp. 89-101.

Kurihara, Y., R. Tuleya and M. Bender. The GFDL Hurricane Prediction System and Its Performance in the 1995 Hurricane Season. *Monthly Weather Review*, Vol. 126, Issue 5, pp.1306-1322.

Lee, W-C and M.M. Bell, 2007: Rapid intensification, eyewall contraction and breakdown of Hurricane Charley (2004) near landfall. *Geophys. Res. Lett.*, 34, L02802, doc:10.1029/2006GL027889.

Powell, M., 2007: New findings on hurricane intensity, wind field extent and surface drag coefficient behavior. 10<sup>th</sup> International Workshop on Wave Hindcasting and Forecasting and Coastal Hazard Symposium, North Shore, Hawaii, November 11-16, 2007.

Tropical Prediction Center, 2005. Tropical Cyclone Report Hurricane Katrina. <http://www.nhc.noaa.gov/>

Ullhorn, E. W. and P. G. Black, 2003: Verification of remotely sensed sea surface winds in hurricanes. *J. Atmos. Oceanic Technol.*, 20-99-116.

Ullhorn, E. W., P. G. Black, J. L. Franklin, M. Goodberlet, J. Carswell and Alan Goldstein, 2006: Hurricane surface wind measurements from an operational stepped frequency microwave

radiometer. Submitted to *Monthly Weather Review*.

Vickery, P. J. P.F. Skerlj, A.C. Steckley and L. A. Twisdale, 2000: Hurricane wind field model for use in hurricane simulations. *J. of Structural Engineering*. 1203-

Vickery, P. J., 2005: Simple empirical models for estimating the increase in the central pressure of tropical cyclones after landfall along the coastline of the United States. *J. of Appl. Meteor.*, 44, 1807-1825.

Vickery, P. J. and P. F. Skerlj, 2005: Hurricane gust factors revisited. *J. of Structural Engineering*, (May), 825-832.

Vickery, P., 2007: Uncertainty in population properties of North Atlantic tropical cyclones. 10<sup>th</sup> International Workshop on Wave Hindcasting and Forecasting and Coastal Hazard Symposium, North Shore, Hawaii, November 11-16, 2007.

WAMDI Group, 1988. The WAM model - a third generation ocean wave prediction model. *J. Phys. Ocean.* 18: 1775-1810.

Willoughby, H. E. and M. E. Rahn, 2004: Parametric representation of the primary hurricane vortex, Part II: Observations and evaluation of the Holland (1980) wind model. *Mon. Wea. Rev.*, 132, 3033-3048.

Willoughby, H. E. and M. E. Rahn, 2004: Parametric representation of the primary hurricane vortex, Part I: A new family of sectionally continuous profiles. *Mon. Wea. Rev.*, 134, 1102-1120.

Wimmers, A. J. and C. Velden, 2007: MIMIC. A new approach to visualizing satellite microwave imagery of tropical cyclones. *B. Amer. Met. Soc.*, (August).